Int. J. Electrochem. Sci., 10 **(2015)** 4155 - 4164

International Journal of
ELECTROCHEMICAL
SCIENCE
www.electrochemsci.org

A PDMS Microfluidic Impedance Immunosensor for Sensitive Detection Of Pesticide Residues in Vegetable Real Samples

Yemin Guo[1], *Xianfu Liu*[2], *Xia Sun*[1,*], *Yaoyao Cao*[1], *XiangYou Wang*[1,*]

[1]School of Agriculture and Food Engineering, Shandong University of Technology, No. 12, Zhangzhou Road, Zibo 255049, Shandong Province, P. R. China
[2] Shandong Insitute of Scientific and Technical Information, No. 607 Shunhua Road, Jinan 250101, Shandong Province, P. R. China
[*]E-mail: sunxia2151@sina.com; wxy@sdut.edu.cn

Received: 9 February 2015 / *Accepted:* 12 March 2015 / *Published:* 23 March 2015

In this article, a poly (dimethylsiloxane) (PDMS) microfluidic immunosensor chip with embedded gold interdigitated array microelectrode (IDAM) was used for constructing an immunosesor to rapidly detect pesticide residues in vegetable real samples. This microfluidics chip consisted of a detection microchamber inlet and outlet microchannel. Using chlorpyrifos as the model compound, anti-chlorpyrifos monoclonal antibodies were orientedly immobilized onto the IDAM surface through protein A. The detection microchamber with a dimension of 6mm×0.5mm×0.02mm and a volume of 60 nL was used to collect chlorpyrifos, which was captured by antibody immobilized on IDAM to produce a sensitive impedance change. Electrochemical impedance spectroscopy (EIS) was used in conjunction with the fabricated sensor to detect chlorpyrifos. Parameters affecting the microfluidic immunosensor chip response such as velocity and rate of flow in microchannel, antibody loading and incubation time were optimized. Under the optimum condition, this microfluidic immunosensor possessed a wider range, better reproducibility , higher stability and lower detection limit, . Meanwhile, the proposed microfluidic immunosensor can also be employed for directly analyzing practical samples. This will be a new promising tool in the process of pesticide residue analysis.

Keywords: microfluidic chip; immunosensor; pesticide residue; rapidly detection.

1. INTRODUCTION

Because of their high efficiency, pesticides as insecticides are widely adopted in modern agriculture [1]. Unfortunately, these compounds had high acute toxicity, they were harmful to human health and the environment [2]. So rapid detection and reliable quantification of pesticide have become increasingly of importance for public security and health protection [3,4]. Compared with traditional methods for the determination of pesticide residues, electrochemical immunosensors exhibit the

following advantages, such as rapid response, simple instrumentation, easy operation, high sensitivity, selectivity and high compatibility with advanced micromachining technologies and nanotechnology [5-8]. Microelectrodes that were fabricated adopting lithographic techniques have been interesting because they typically have higher sensitivities than macroelectrodes. Macroelectrodes have a semi-infinite linear diffusion profile leading to a greater depletion of reactants in contrast to the microelectrodes which have spherical diffusion profile satisfying a greater rate of reactant supply [9]. Among microelectrodes, interdigitated array microelectrodes (IDAM) show promising advantages in terms of fast establishment of steady-state, low ohmic drop, , increased signal-to-noise ratio, and rapid kinetics of reaction [10,11].In order to further improve the capabilities of IDAM in impedance sensing, microfluidic flow cells can be constructed in the IDAM to acquire a fully integrated microchip for broad applications including impedance detection and dielectrophoresis [12,13]

Employing high performance, design flexibility, reagent economy, high throughput, miniaturization, and automation, microfluidic analysis systems is becoming a powerful tool in chemical and biological assays. [14]. Therefore, the new device that combined microfluidic flow cells with embedded IDAM presents high detection sensitivity, small volume processing, low contamination during bacterial growth, and rapid detection of small number of cells. Due to increase of the surface to volume ratio and decrease of the distance that conductive ions diffuse to reach the sensor surface in the new device , a rapid kinetic reaction was achieved [15]

In this study, we aimed to obtain a detection method possessing high sensitivity, smaller reagent consumption, miniaturization, and automation. Microfluidic analysis systems with embedded gold interdigitated array microelectrode can satisfy these requirements. To date, however, the application of microfluidic immunosensor chip by orientedly immobilizing antibody onto the embedded IDAM for pesticide residues detection has been still very less reported. In this study, we want to make use of the advantages of i microfluidic flow cells with embedded IDAM to reduce the amount of reagent, especially expensive antibody and improve the detection sensitivity. At the same time, anti-chlorpyrifos monoclonal antibodies were orientedly immobilized onto the IDAM surface through protein A. This microfluidics chip consisted of a detection microchamber inlet and outlet microchannel. The sample was captured by antibody immobilized on IDAM to produce a sensitive impedance change. The impedance change was calculated to quantitative analysis pesticide residues in vegetable and fruit samples.

2. MATERIALS AND METHODS

2.1 Reagents

Anti-chlorpyrifos monoclonal antibody, chlorpyrifos were all purchased from Lifeholder (Sunbiotech Co., Beijing, China). Protein A and bovine serum albumin (BSA, 96-99%) were all purchased from Sigma (Sigma Diagnostics Co., Missouri, USA). The ultrapure water (18.2 MΩ • cm) was produced by Zahner (Millipore Co., Hessen, Germany) was used throughout.

2.2 Apparatus

We performed impedance measurements using an IM-6 impedance analyzer (BAS, West Lafayette, IN) with IM-6/THALES-software. A sine-modulated AC potential of 100mV was applied across the IDAM for all impedance measurements. Meahwhile we measured the magnitude and phase angle of impedance under a frequency range from 10 Hz to 1 MHz. One electrode of the IDAM chip was connected to the test probes, and the other two were connected to the reference electrode and counter one of the impedance analyzer.

2.3 Fabrication of the microfluidic flow cell with embedded IDAM

We fabricated the microfluidic flow cell with embedded IDAM according to the procedure prescribed by Varshney et al., [16]. The structure of the new device is shown in Fig. 1. Each IDAM chip was made up of 50 pairs of Au interdigitated electrode fingers with a finger width of 25 μm and a gap of 25μm. PDMS microchannel and SU-8 mould were constructed based on the steps suggested by Pooran et al.[17]. The microchannel has a detection microchamber with its size of 6mm×0.5mm×0.02mm and volume of 60 nL (Fig. 1).

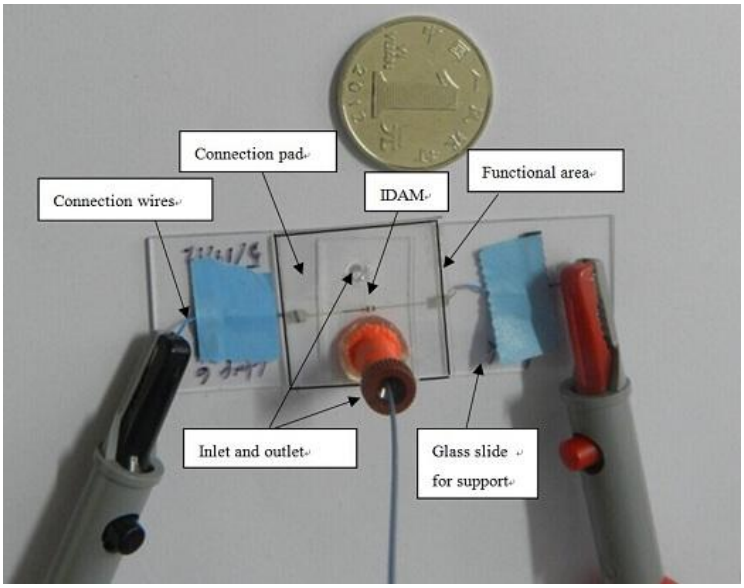

Figure 1. Strucute of an assembled microfluidic flow cell integrating with embedded IDAM and connection wires.

2.4 Preparation of microfluidic immunosesor and impedance measurements

After each test, the flow cell was flushed with 0.1M sodium hydroxide for 1 h, double distilled water for 30 min, 0.1M hydrochloric acid for 1 h, and a final rinse with double distilled water for 30 min. The flow rate for flushing was set at 10μL/min. All impedance measurements were performed in the presence of 10 mM $[Fe(CN)_6]^{3-/4-}$ (1:1) mixture in PBS (pH 7.5) as a redox probe. Determining

frequency associated with the largest difference in absolute impedance between the vegetable sample and the control one, a curve was plotted between normalized impedance change (NIC) and frequency. The impedance measurements process was following:

1. Immobilized antibody in the micro fluidic chip, washed with PBS for 10 minutes, then detected the impedance, obtained the value $Z_{control}$ of impedance by using the Bode curve in the impedance spectra.

2. Add fruits and vegetables sample liquid, microfluidic chip flushing with 10min PBS after impedance detection, using the impedance was obtained in the Bode curve,obtaining the impedance value Z_{sample};

3. Calculated the impedance change (Z_{sample}-$Z_{control}$) exposure to pesticide before and after, then obtained the actual sample concentration of pesticide according to the relation curve of impedance changes with the concentration of chlorpyrifos.

NIC can be calculated with the following equation:

$NIC=(Z_{sample}-Z_{control})/Z_{control}\times 100\%$

2.5 Preparation and determination of real vegetable samples

Vegetable samples (leek, lettuce and cabbage) for detection study were purchased from the local supermarket and rinsed thoroughly with distilled water. The samples were dried in the air and chopped into 3×3 mm particles approximately. Different concentrations of chlorpyrifos solutions were sprayed on their surfaces respectively. After equilibration for 3 h at room temperature to allow pesticide absorptioninto the samples, a mixture of 1 mL acetone and 9 mL 0.1M phosphate buffer (pH 7.4) was sprayed onto each sample weighing 10 g. After treated in ultrasonic for 15 min, the suspensions were centrifuged for 10 min at 2000 rpm. The precipitate at the bottom of the centrifuge tube was removed. Then the clear supernatant extract was analyzed for pesticide inhibition by employing the obtained immunosensor detection method.

3. RESULTS AND DISCUSSION

3.1 Impedance characterization of the modifying process

Figure 2 presented the magnitude and phase angle of the impedance spectra in the condition of $[Fe(CN)6]^{3-/4-}$ as the redox probe in PBS. The frequency range was from 10 Hz to 1 MHz. Each step was measured three times. The impedance magnitude shows the contributions of the capacitive and resistive portions to the phase angle. We can find that the capacitive portion of impedance is determinative at the high side and low side of the frequency range and the resistance portion of impedance is determinative at the scope of mid frequency. As shown in the Fig.2, in the frequency scope from 10 Hz to 1 MHz, the magnitude of impedance increased with the steps of (a) the bare microfluidic chip, (b) 100 μg/mL protein A modification, (c) 100 μg/mL anti-chlorpyrifos antibody immobilization, (d) 100 ng/mL chlorpyrifos bound microfluidic chip. With frequencies higher than 10

kHz, no significant difference was observed between spectra a, b, c,and d. This situation was caused by hindering the transmission of electrons toward the electrode surface.

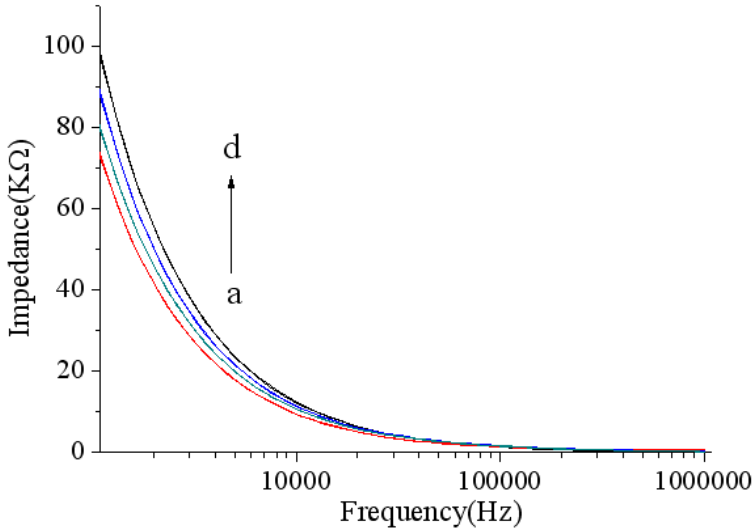

Figure 2. Bode amplitude curves of impedance spectra (a) bare microfluidic chip (b) 100 μg/mL protein A modification; (c) 100 μg/mL anti- chlorpyrifos antibody immobilization; (d) 100 ng/mL chlorpyrifos bound micorfluidic chip with [Fe(CN)6]3-/4- as the redox probe in PBS. Scope of Frequency (10 Hz--1MHz）. Working voltage-- 100 mV.

3.2 Optimization parameters of the experimental conditions

3.2.1 Influence of the feeding speed of the micropump

The feeding speed of the micropump had significant effects on the impedance of the testing liquid during the process of the liquid fed into the microfluidic chip. When the feeding speed of the pump was low, the flow rate of test liquid was low too. When the feeding speed of the pump increased, the pressure of liquid in the channel increased and the impedance of the test liquid increased meanwhile as shown in Fig. 3A. There existed a linear relationship between the feeding speed and the impedance of the liquid. Taken the service life of the microfluidic chip, 10μL/min was set as a flow rate.

3.2.2 Influence of the applied working voltage on the impedance analyzer

The impedance values were principally determined by the nature of the testing solution during the different voltages. When the working voltage was changed, the impedance value had almost no change at all, but it tended to a stable value as shown in Fig. 3B. Considering that 100 mV can maintain linear measurement for the impedance and overcome the noise, so 100 mV was set as external applied voltage in this experiment.

3.2.3 Influence of the feeding time of the micropump

The volume of the testing liquid fed into the chip had some influence on the impedance. The volume of the testing liquid was increased along with the increase of time that the liquid was fed into the chip by the micropump. The volume of the liquid increased with the increase of feeding time during the period of 1 to 10 minutes and the impedance increased at the same time. If the feeding time exceeded 10 minutes, the impedance had little change and tended to a stable state. 10 minutes was selected as feeding time of the micropump.

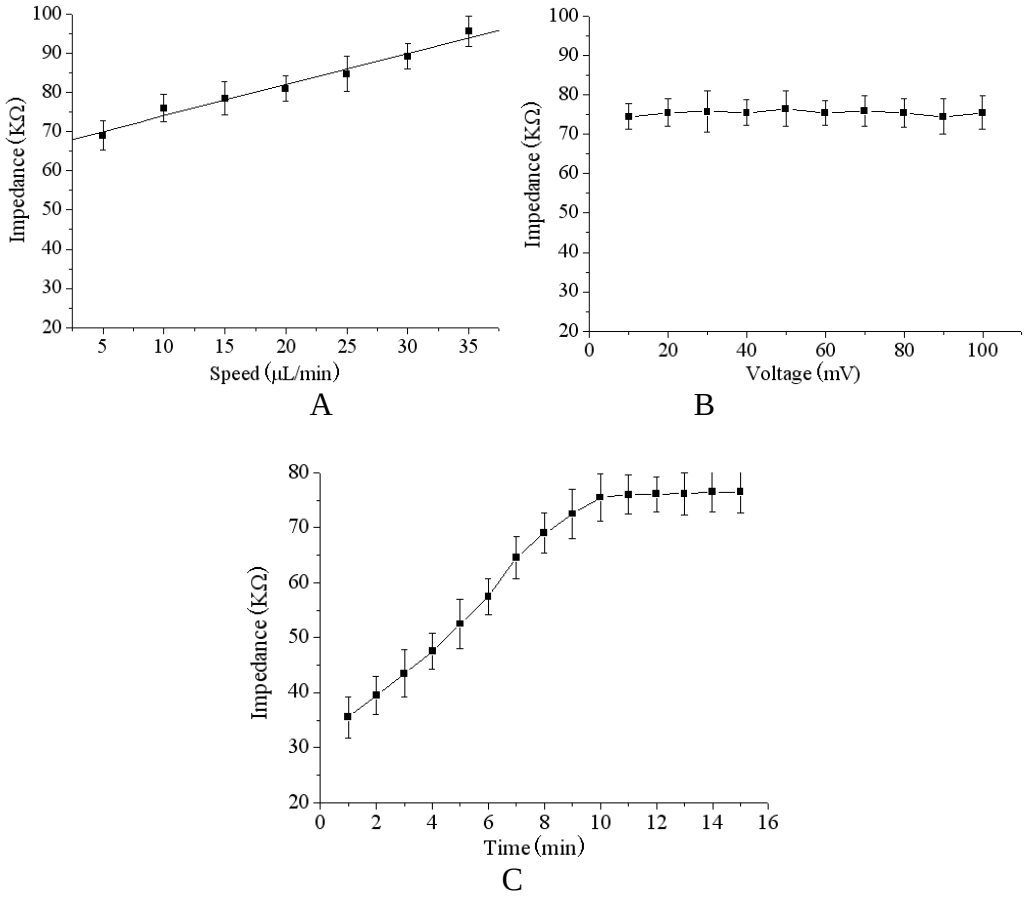

Figure 3. Experiment parameters optimization : (A)Feeding speed of the micropump; (B)The applied voltage on the impedance analyzer; (C) Feeding time of the micropump.

3.3 Calibration curve for chlorpyrifos detection

The Bode amplitude plots of impedance spectra were performed before and after exposure to different concentrations of pesticides (Fig. 4A). As it shown in the Fig. 4A, the impedance values in the presence of chlorpyrifos was increased obviously than that in the absence of chlorpyrifos, and larger and larger with the increasing concentrations of chlorpyrifos. Under optimal experimental conditions, the calibration curve for detecting chlorpyrifos with the proposed aptasensor is shown in Fig. 4B. A good linear relationship between the relative current change and logarithm of chlorpyrifos

concentration in the range from 10 to 10^5 ng/mL was obtained. The linear regression equation is ΔZ=9.84+65.58lgC (ng/mL) with the correlation coefficients of 0.9762. The detection limit was calculated to be 1 ng/mL at a signal/noise ratio of 3 (S/N=3) between the detection signal of low concentration samples and the noise of blank ones, which is lower than that of other chlorpyrifos detection methods showed in Table 1. As comparison, the gold interdigitated array microelectrode (IAM) was used for chlorpyrifos detection in our group. As shown in Table. 1, compared with PDMS Microfluidic, the liner range of IAM was narrow, although the detection limit of IAM was slightly higher.

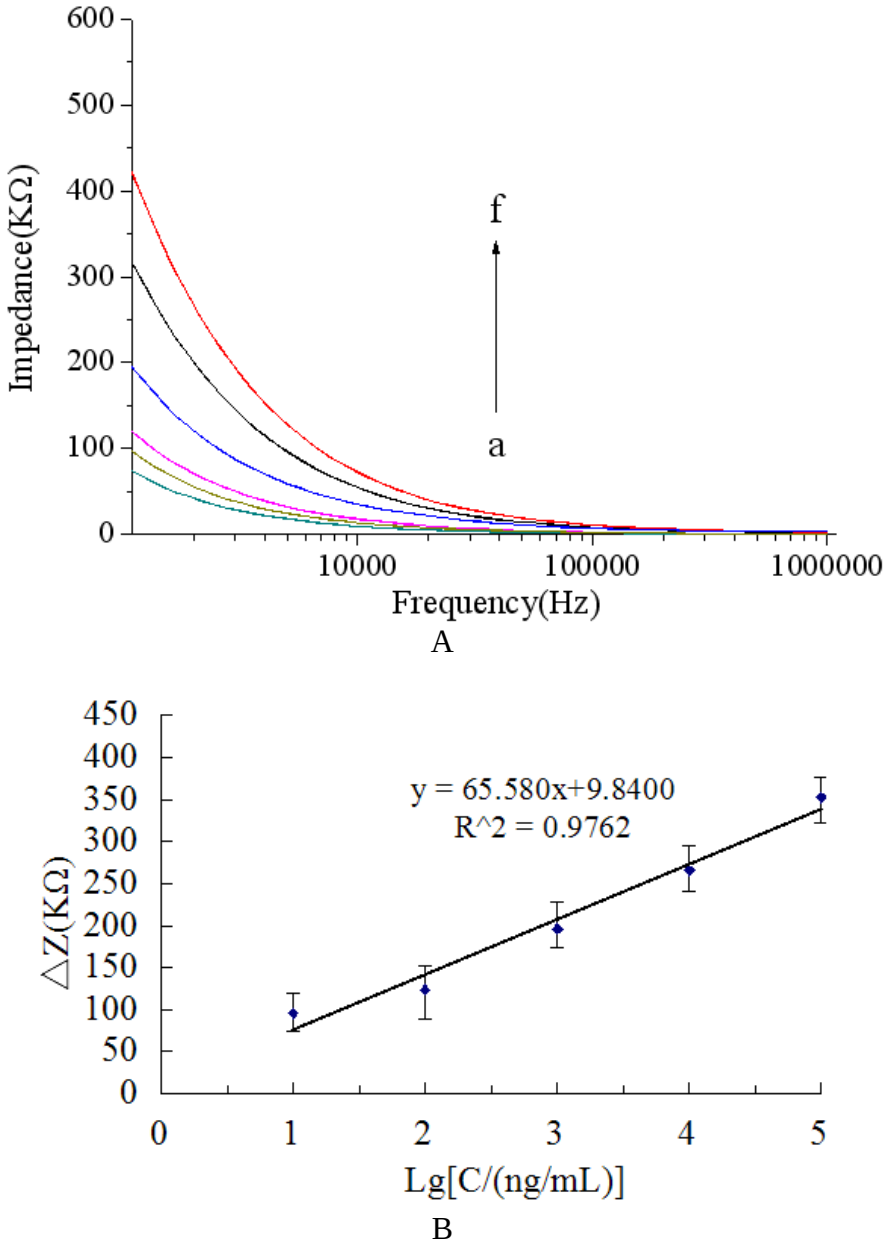

Figure 4. (A) Bode amplitude plots of impedance spectrawith $[Fe(CN)6]^{3-/4-}$ as the redox probe in PBS after inhibition with chlorpyrifos for 10 min. Chlorpyrifos concentration (a)–(f):0, 1, 10, 10^2, 10^3, 10^4, 10^5ng/mL. (B)Calibration curve of the relative current changes (ΔZ) of the suggested microfluidic immunosensor versus the logarithm of *chlorpyrifos* concentration.

Table 1. Comparison with other analytical methods for the determination of chlorpyrifos.

Method of detection	Detection limit (ng/mL)	Liner range (ng/mL)	References
immunochromatography	132.91	50-12150	[18]
AChE-[BMIM][BF_4][a]-MWCNT/CP[b]	1.4	3.5-350	[19]
Nafion/AChE/CHIT/IAM	0.78	1-100	[20]
PDMS Microfluidic Impedance Immunosensor	1	10-10^5	this work

3.4 Performance of the microfluidic immunosensor

That the impedance between the bare electrodes after cleaning the modified microfluidic chip can be restored to the original data illustrated that the chip had higher repetition utilization. On the other hand, the impedance values did not change significantly (see Fig. 5) after conduct 10 repeat tests on the impedance in microfluidic chip. This meant that the chip had good stability.

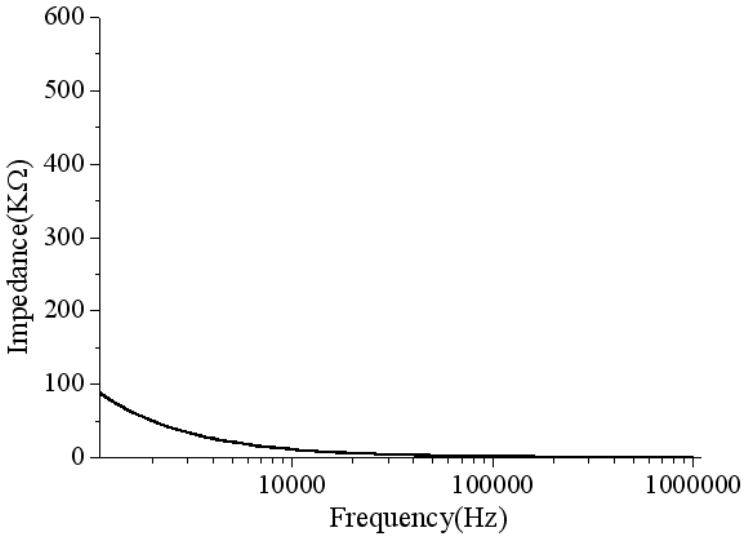

Figure 5. 10 Repeat tests on the microfluidic chip after antibody modification

3.5 Determination of chlorpyrifos in vegetable samples

Vegetable samples (leek, lettuce and cabbage) for detection study were purchased from the local supermarket and flushed thoroughly using distilled water. Then the vegetables were dried in the air and chopped into 3×3 mm particles approximately. Different concentrations of chlorpyrifos solution were sprayed onto their surfaces. As displayed in Table 2, the recovery tests were conducted using 3 replicates with the microfluidic immunosensor that prepared in the same way. Then the recovery rate of 88.6~102.5% shown that the microfluidic immunosensor was effective for the analysis of chlorpyrifos in vegetable samples.

Table 2. Determination of chlorpyrifos in vegetable samples

Sample	Added (ng/mL)	Found (ng/mL)	RSD (%) (n=3)	Recovery (%)
leek	10	9.13	3.44	91.3
	1.0×10^2	0.94×10^2	3.82	94.0
	1.0×10^3	1.025×10^3	4.56	102.5
lettuce	10	9.63	5.10	96.3
	1.0×10^2	0.886×10^2	4.99	88.6
	1.0×10^3	0.897×10^3	3.34	95.0
pakchoi	10	9.65	4.51	96.5
	1.0×10^2	0.942×10^2	5.27	94.2
	1.0×10^3	0.951×10^3	4.93	95.1

4. CONCLUSIONS

In this paper, we took advantage of integrating microfluidic flow cells with embedded IDAM to fabricate immunosensor for rapidly detecting pesticide residues in vegetable real samples. This microfluidics chip consisted of a detection microchamber inlet and outlet microchannel. Using chlorpyrifos as the model compound, anti-chlorpyrifos monoclonal antibodies were orientedly immobilized onto the IDAM surface through protein A. Under the optimum condition, this microfluidic immunosensor showed a wider range, lower detection limit, better reproducibility and higher stability. Compared with the traditional immunosensor detection methods, the integrated microfluidic immunosensor needed a small number of sample to conduct faster detection. Due to its wider applications in many fields, miniaturized immunosensors will make a great contribution to faster, more accurate and direct analysis of pesticide residues in vegetable real samples.

ACKNOWLEDGEMENTS
This work was supported by the National Natural Science Foundation of China (No.30972055, 31101286, 31471641), Agricultural Science and Technology Achievements Transformation Fund Projects of the Ministry of Science and Technology of China (No.2011GB2C60020), Special project of independent innovation of Shandong Province (2014CGZH0703) and Shandong Provincial Natural Science Foundation, China (No.Q2008D03, ZR2014CM009).

References

1. J. Vymazal, T. Březinová, *Environment International*, 75 (2015) 11
2. N. Chauhan, C. S. Pundir, *Electrochimica Acta*, 67 (2012) 79
3. J. Gong, Z. Guan, D. Song, *Biosens Bioelectron.*,39 (2013) 320
4. X. Sun, X. Wang, *Biosens Bioelectron.*, 25 (2010) 2611
5. E.P. Syrago-Styliani, G. Evagelos, T. Anthony, A.S. Panayotis, *J. Chromatogr. A*, 1108 (2006) 99
6. J. Zhu, M. Jin, W. Gui, Y. Guo, R. Jin, C. Wang, *Food Chem.*, 107 (2008) 1737
7. T. Liu, H. Su, X. Qu, P. Ju, L. Cui, S. Ai, *Sens. Actuators B:Chem.*, 160 (2011) 1255
8. X. Jiang, D. Li, X. Xu, Y. Ying, Y. Li, Z. Ye, J. Wang, *Biosens. Bioelectron.*, 23 (2008) 1577

9. M. Varshney, Y. Li, B. Srinivasan, S. Tung, *Sensors and Actuators B*, 128 (2007) 99
10. C. Amatore, B. Fosset, *J. Electroanal.Chem.*, 256 (1988) 255
11. M. Ciszkowska, Z. Stojeck, J. Electroanal. Chem., 466(1999) 129
12. B. Chang, C. Chen, S. Ding, D. Chen, H. Chang, *Sens. Actuators B: Chem.*, 105 (2005) 159
13. R. Zhou, P. Wang, H. Chang, *Electrophoresis*, 27 (2006) 1376
14. H. Wang, S. Meng, K. Guo, Y. Liu, P. Yang, W. Zhong, B. Liu, *Electrochemistry Communications*, 10 (2008) 447
15. S.K. Kim, P.J. Hesketh, C. Li, J.H. Thomas, H.B. Halshall, W.R. Heineman, *Biosens. Bioelectron.*, 20 (2004) 887
16. M. Varshney, Y. Li, *Biosens. Bioelectron.*, 22 (2007) 2408
17. R. Pooran, S. Tung, J.W. Kim, *Proceedings of the IEEE International Conference on Micro Electro Mechanical Systems* (2005) 37
18. 18. X.D. Hua, G.L. Qian, J.F. Yang, B.S. Hu, J.Q. Fan, N. Qin, G. Li, Y.Y. Wang and F.Q. Liu, *Biosens. Bioelectron.*, 26 (2010) 189
19. L.G. Zamfir , L. Rotariu , C. Bala, *Biosens Bioelectron.*, 26 (2011) 3692
20. Z. Gong, Y. Guo, X. Sun, Y. Cao, X. Wang, *Bioprocess Biosyst Eng.*, 37(2014)1929.